Supplementary Information for

A Self-Defense Redox Mediator for Efficient Lithium-O_2 Batteries

Tao Zhang,[a] Kaiming Liao,[a] Ping He[b] and Haoshen Zhou[a,b]*

[a]Energy Technology Research Institute, National Institute of Advanced Industrial Science and Technology (AIST), Umezono 1-1-1, Tsukuba, 305-8568, Japan

[b]National Laboratory of Solid State Microstructure, College of Engineering and Applied Sciences, Nanjing University, Nanjing, 210093, P. R. China

To whom correspondence should be addressed. E-mail: hs.zhou@aist.go.jp

Calculation of Cations' Effective Reduction Potential

Nernst equation:

$$E_{Red} = E_{Red}^{0} - \frac{RT}{zF}\ln\frac{a_{Red}}{a_{Ox}} \qquad (1)$$

Where R is the universal gas constant (8.314462 J/K·mol), T is the absolute temperature (273.15 + 25 = 298.15 K in this work), and α is the chemical activity for the relevant species (a_{Red} is for the reduced state and a_{Ox} is for the oxidized state). F is the Faraday constant (96485.3365 C/mol), and z is the number of moles of electrons transferred based on the reaction of $a_{Ox} + ze^{-} = a_{Red}$. Note that $a_j = \gamma_j Cj$, where γ_j and Cj are the activity coefficient and the concentration of species j. In a diluted solution with low concentration for the selected metallic cations, a_j can be simplified to equal the concentration Cj, and then Eq. (1) can be simplified as:

$$E_{Red} = E_{Red}^{0} - \frac{0.05916}{z}\log_{10}\frac{1}{a_{Ox}} \qquad (2)$$

According to Eq. (2), the effective reduction potential of the In^{3+} ions in the Li-O_2 cell containing 16.7 mM InI_3 is calculated as -0.375 V.

According to the same Eq. (2), the effective reduction potential of the Li^{+} ions in the Li-O_2 cell containing 50 mM LiI is calculated as -3.058 V.

Supplementary Figures

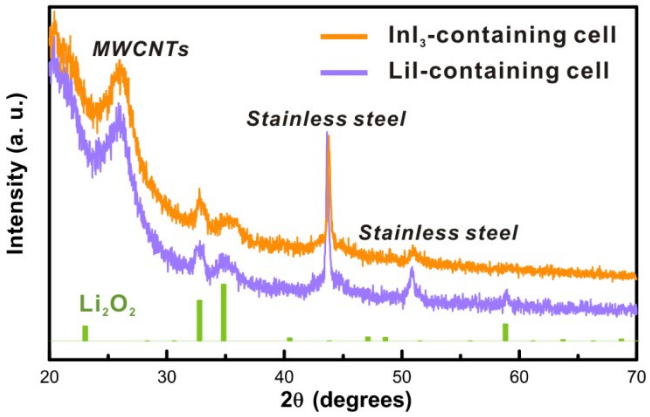

Supplementary Fig. S1 XRD patterns of the MWCNTs cathodes in discharge state. The MWCNTs cathodes were taken out from the LiI- and InI_3-containing Li-O_2 coin cells, respectively. The cathodes with the stainless steel current collector were washed by super-anhydration acetonitrile and then dried before the XRD measurement.

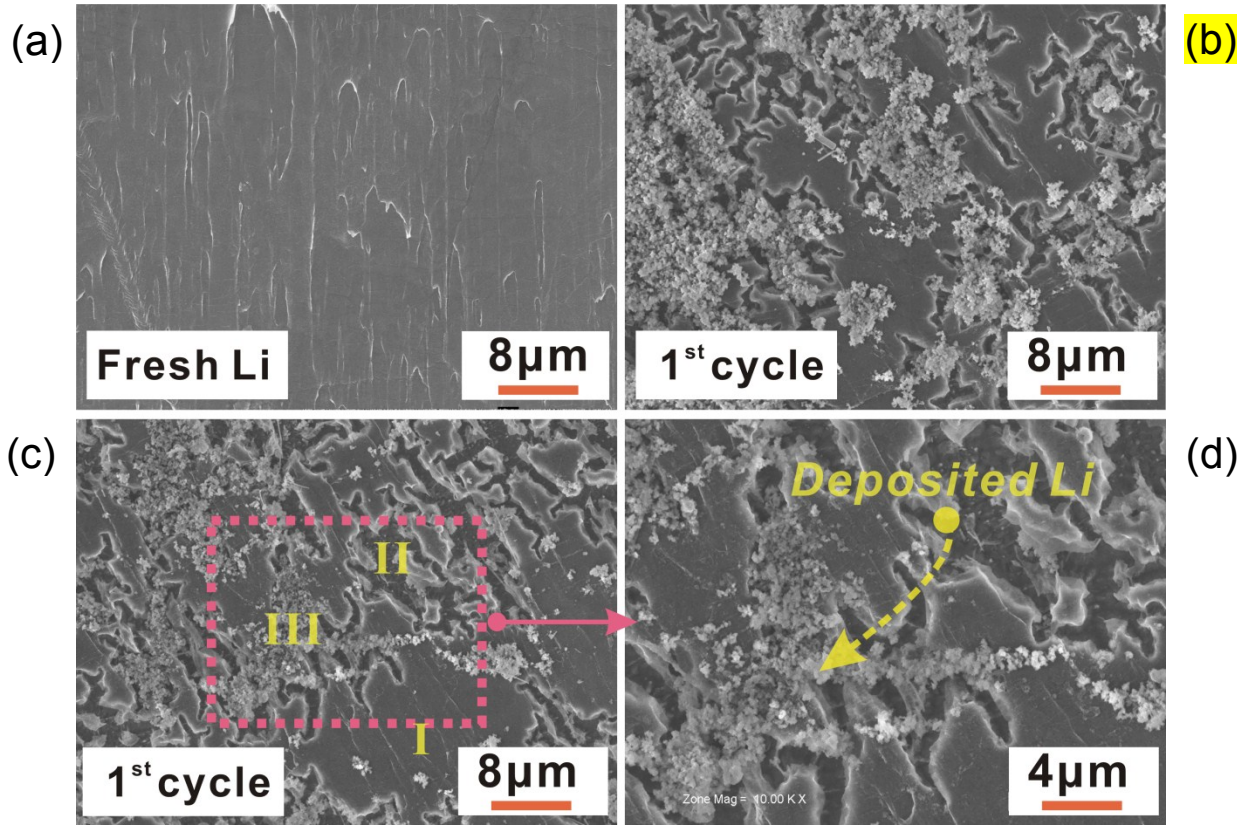

Supplementary Fig. S2 Magnification of SEM images (a) the surface of a fresh Li anode, corresponding to *Fig. 4b*. (b) The neighbouring area of *Fig. 4c*. (c) and (d) the surface of Li anode in the LiI-containing cell after the first cycle, corresponding to *Fig. 4c*.

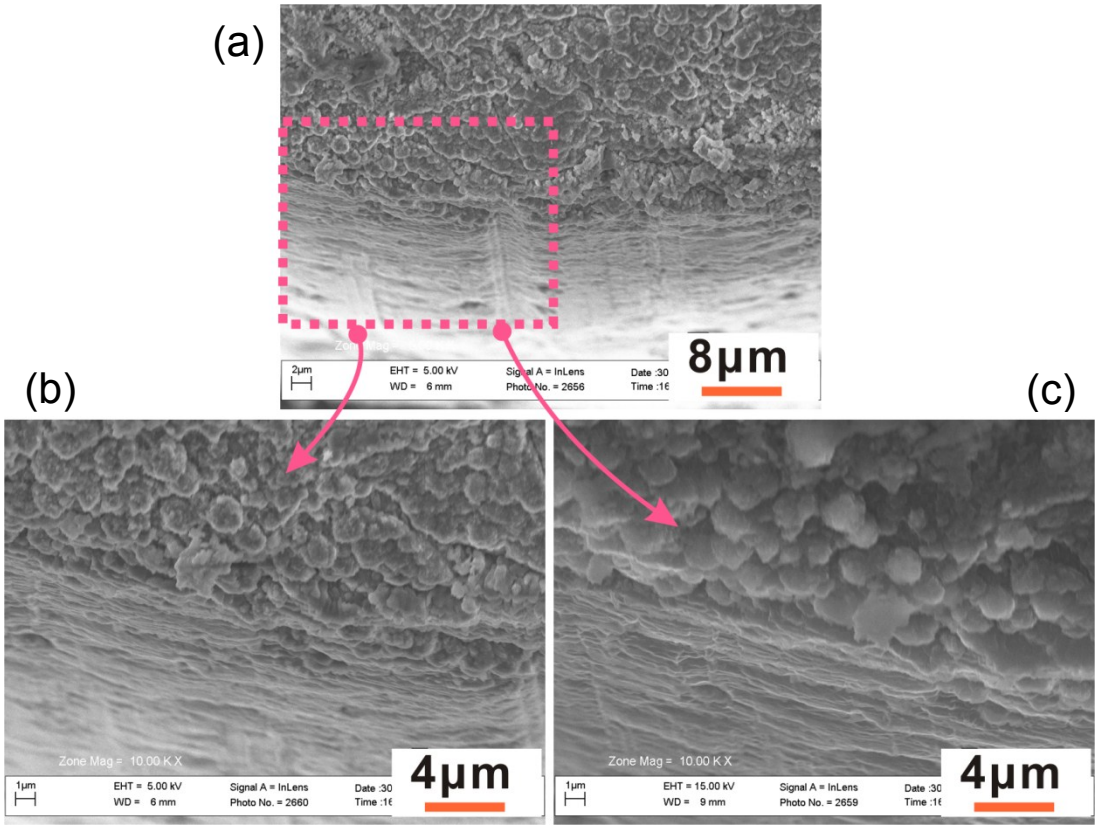

Supplementary Fig. S3 Magnification of SEM images, corresponding to *Fig. 4f*. (b) and (c) are obtained from the observations for the same area in (a). The EHT (extra high tension) values performed are different: 5.00 kV for (b) and 15.00 kV for (c), to focus clearly on the surface area for (b) and the cross section area for (c).

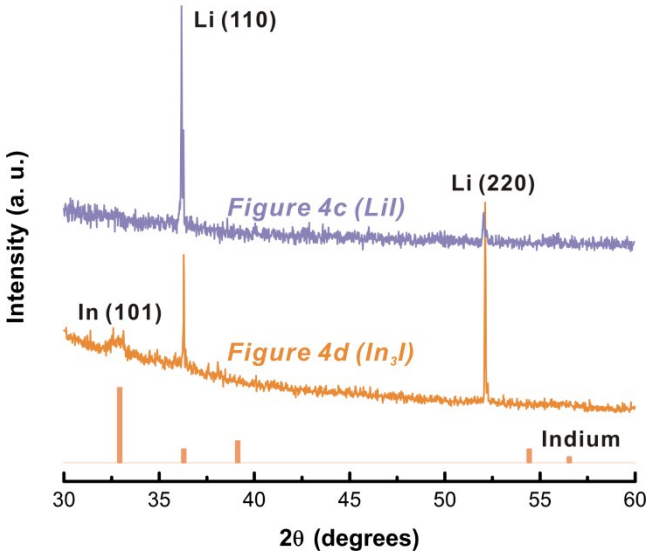

Supplementary Fig. S4 Close examination of the XRD patterns shown in *Fig. 4g*. The two patterns are corresponding to the Li anode in the LiI- and In_3I-containing cells after the first cycle, as shown in *Fig. 4c* and *Fig. 4d*, respectively. The reference XRD pattern of indium is also shown (PDF no. 65-9682).

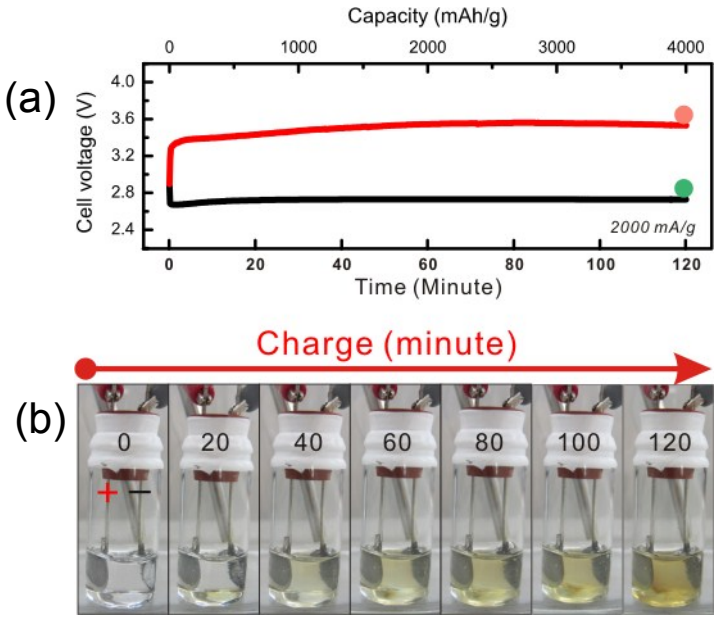

Supplementary Fig. S5 A visual Li-O_2 beaker cell with the InI_3-containing electrolyte. (a) Charge curve of the visual Li-O_2 beaker cell at 2000 mA/g in 1 atm pure O_2. The beaker cell consists of a MWCNTs cathode in discharged state (4000 mAh/g), a fresh lithium anode and an electrolyte of 16.7 mM InI_3, 0.5 M $LiClO_4$ in DMSO. (b) Visual observation of the Li-O_2 beaker cell recorded as charging proceeds.

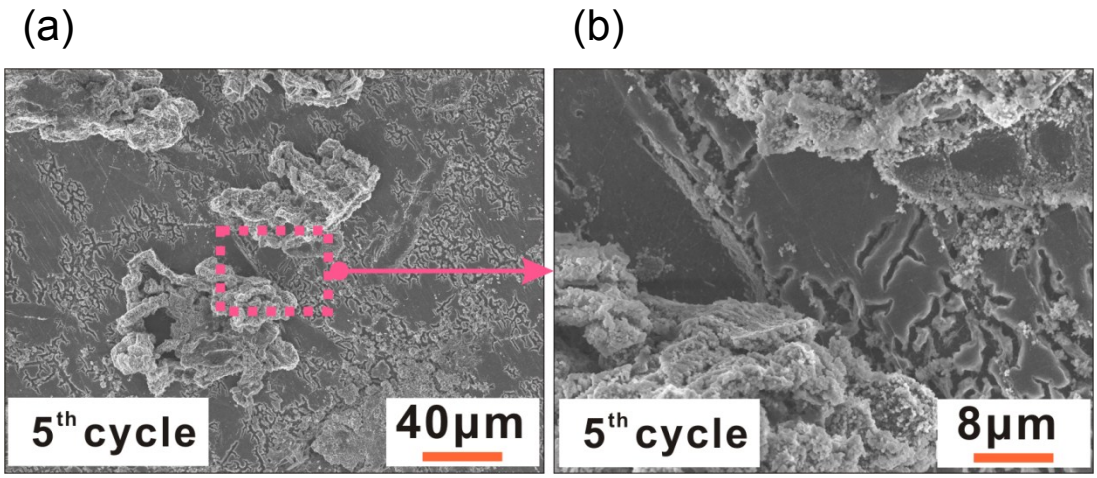

Supplementary Fig. S6 Micrograph images showing the growth of protrusions from the Li anode. Both (a) and (b) are corresponding to *Fig. 6b*. The Li anode was taken out from a LiI-containing Li-O_2 cell after five cycles at 500 mA/g.

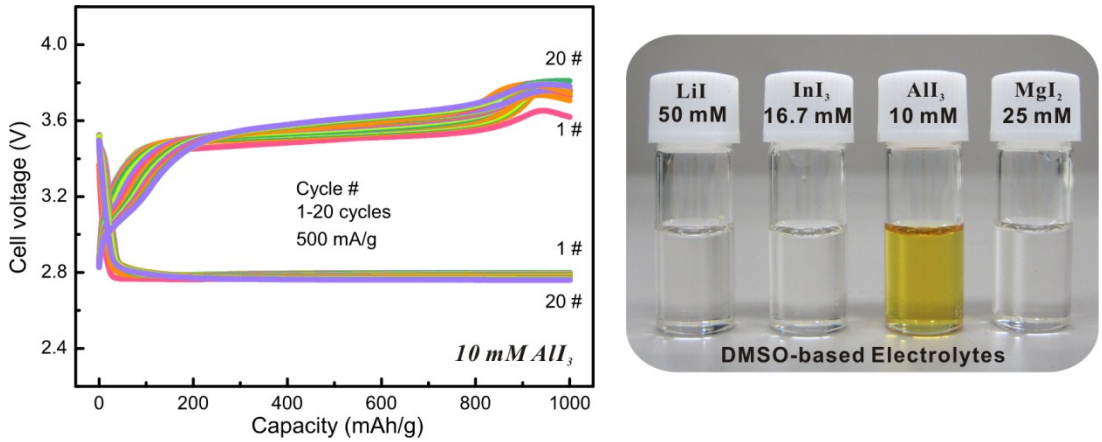

Supplementary Fig. S7 Discharge/charge behavior of Li-O_2 cells with 10 mM AlI_3 in DMSO. On the right is a picture of the DMSO-based electrolytes containing 50 mM LiI, 16.7 mM InI_3, 10 mM AlI_3 and 25 mM MgI_2, respectively.

According to Eq. (2), the effective reduction potential of the Al^{3+} ions in the Li-O_2 cell containing 10 mM AlI_3 is calculated as -1.715 V.

The AlI_3-containing cell exhibits considerably smooth charge curves. However, unlike LiI, InI_3 and MgI_2, the AlI_3 has low solubility (no more than 10 mM) and is prone to decompose in the DMSO electrolyte.

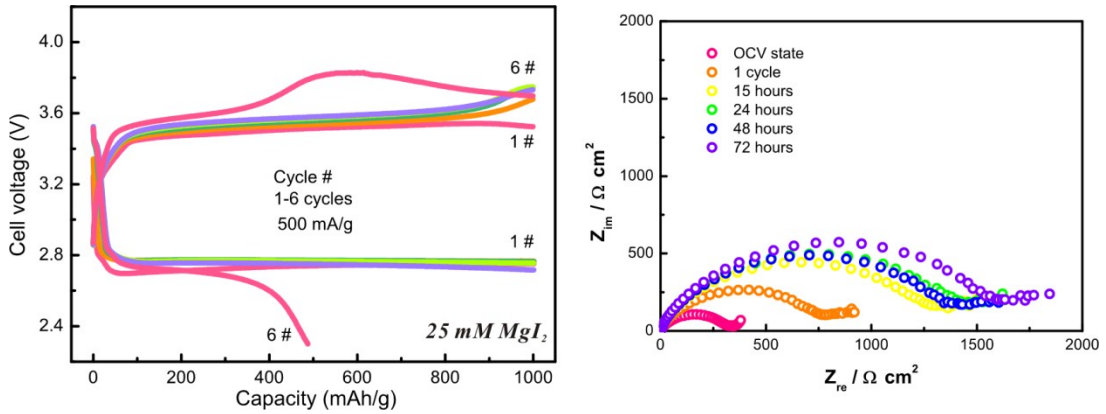

Supplementary Fig. S8 Discharge/charge curves of Li-O_2 cells with 25 mM MgI_2 in DMSO. On the right is the variation of impedance spectra on discharging and charging the MgI_2-containing Li-O_2 cell for one cycle and then keeping for 72 hours.

According to Eq. (2), the effective reduction potential of the Mg^{2+} ions in the Li-O_2 cell containing 25 mM MgI_2 is calculated as -2.403 V.

The solubility and stability of MgI_2 in DMSO are comparable to InI_3, but the impedance of the MgI_2-containing Li-O_2 cell increased gradually as keeping. Such phenomenon was not observed for all of the LiI-, InI_3- and AlI_3-containg Li-O_2 cells. When exposed to air, a thin layer of oxide is generally formed on the surface of metallic magnesium, which is fairly impermeable. We speculated that that a compact passivation film may exist on magnesium surface layer, hindering the charge transfer and leading to poor cycling performance.